frontiers | Frontiers in Energy Research

TYPE Brief Research Report
PUBLISHED 17 November 2025
DOI 10.3389/fenrg.2025.1693639

OPEN ACCESS

EDITED BY
Xiangyu Zhang,
North China Electric Power University, China

REVIEWED BY
Linfei Yin,
Guangxi University, China
Yulian Jiang,
Changchun University of Technology, China
Rongpeng Liu,
McGill University, Canada

*CORRESPONDENCE
Sheng Chen,
shchen_gzcsg@126.com

RECEIVED 27 August 2025
REVISED 06 October 2025
ACCEPTED 20 October 2025
PUBLISHED 17 November 2025

CITATION
Chen S, Fu T, Lan H, Hao L, Yang Y and Weng Z (2025) A data-driven framework for unit commitment considering ramping and forecasting information.
Front. Energy Res. 13:1693639.
doi: 10.3389/fenrg.2025.1693639

A data-driven framework for unit commitment considering ramping and forecasting information

Sheng Chen[1]*, Tongfu Fu[1], Hai Lan[1], Liping Hao[1], Yanfa Yang[2] and Zehong Weng[2]

[1]China Southern Power Grid Guizhou Power Supply Co., Ltd, Guangzhou, Guizhou, China, [2]Dongfang Electronics Co., Ltd, Yantai, Shandong, China

A data-driven framework was proposed in this paper to enhance the accuracy of load power forecasting and improve the economy and reliability of security-constrained unit commitment (SCUC) scheduling. The loads in each time period are clustered into several distinct scenarios firstly and each scenario exhibits a unique fluctuation boundary, which is quantitatively characterized using the proposed fluctuation indicator. Based on historical data, we evaluated the boundaries of fluctuations at different confidence levels. Then a data-driven framework is proposed to improve the accuracy of evaluating these indices. The effectiveness of this framework is validated using a Long Short-Term Memory (LSTM) network, and the results show that the proposed framework reduced the average error by 45.5% compared to traditional frameworks. Finally, a SCUC optimization model is formulated with these indices results, and case studies were conducted on an IEEE 30-bus system to demonstrate the effectiveness of the proposed method.

KEYWORDS

load clustering, load forecasting, LSTM network, security constrained unit commitment, ramping constraint

1 Introduction

With the rapidly increasing of renewable energy capacity and the development of smart grids, the secure, economical, and reliable operation of power systems has become a critical challenge with considering the operation costs and operation risks (Xu and Zhuan, 2013; Li et al., 2025). As a key component of power system operation, unit commitment (UC) scheduling directly determines the efficiency of power resource allocation and the flexibility of supply-demand balance (Li et al., 2023). Among various scheduling models, security-constrained unit commitment (SCUC) is widely adopted due to its capability of maintaining generation economics and grid security constraints (Fu et al., 2013). However, the accuracy of SCUC scheduling highly depends on the precision of load power forecasting. Accurate load forecasting enables better optimization results of spinning reserve allocation for thermal units, whereas forecasting deviations may lead to power shortages, frequent start-stop cycles of thermal units, and a sharp increase in operating costs (Liu et al., 2025). With the continuous growth in renewable energy penetration and the increasing diversification of user load demands, load power is exhibiting stronger volatility and randomness, which

further enlarges the challenges of load forecasting and poses stricter requirements on traditional SCUC frameworks.

Existing research on load power forecasting has made significant progress through data-driven approaches, such as the application of Gated Recurrent Units (GRU) (Abumohsen et al., 2023) or Long Short-Term Memory (LSTM) networks to capture temporal dependencies in load data (Khuntia et al., 2016). Rafi et al. (2021) developed a hybrid CNN-LSTM model for short-term load forecasting in Bangladesh's power system, which outperformed conventional methods. Wang et al. (2019) used pinball loss with LSTM for probabilistic load forecasting at the consumer level, effectively capturing non-stationary behavior but incurring high computational cost. Zheng et al. (2017) developed a hybrid SD-EMD-LSTM algorithm, which uses XGBoost to evaluate feature importance, applies Empirical Mode Decomposition (EMD) to decompose the load series, and leverages independent LSTM networks to predict individual components before reconstructing the final result. Furthermore, approaches integrating the Attention Mechanism with LSTM networks have demonstrated promising performance in short-term load forecasting in power systems, although they often entail relatively high computational complexity (Lin et al., 2022; Wan et al., 2023). In recent years, researchers have also employed architectures such as the Transformer model and Temporal Convolutional Network (TCN) for time-series forecasting. Wang et al. (2022) proposed a multi-decoder Transformer model (MultiDeT), which effectively captures interactions among multiple energy sources and demonstrates superior prediction accuracy and generalization capability compared to traditional methods. Tian et al. (2024) designed a hybrid CNN-Transformer framework to address probabilistic load forecasting under scenarios with scarce weekend load data. To address industrial load volatility, Wang et al. (2021) proposed a TCN–LightGBM model that achieved significantly lower prediction error than benchmarks in numerical experiments. Meanwhile, Tang et al. (2022) developed an AM-TCN with a channel-temporal dual attention mechanism for dynamic feature weighting, which effectively captured nonlinear meteorological-load relationships on public and utility datasets. While Transformer and TCN models may offer marginal gains in prediction accuracy, they often come with significantly higher computational complexity and training time. Therefore, LSTM remains a highly powerful and popular benchmark model for processing sequential data due to its structural simplicity, effectiveness, and ease of interpretation.

SCUC is a core optimization problem in power system operation and electricity markets. Its objective is to determine the on/off status (0/1 decision) and power output (continuous variable) of each generating unit over a future horizon while satisfying all system security constraints, so as to minimize the total operating cost of the system. Chen et al. (2020) addressed performance optimization of commercial solvers for day-ahead SCUC problems by proposing a distributed optimization framework. This approach combines warm-start and lazy constraint techniques to enhance computational efficiency by leveraging the versatility of solvers such as GUROBI and CPLEX. Fu et al. (2006). Guan et al. (2005) focused on feasibility conditions and corrective scheduling in SCUC. Fu et al. introduced a Benders decomposition-based AC corrective/preventive scheduling model that integrates unit commitment, AC security-constrained optimal power flow (SCOPF), and load shedding, validating the trade-off between system security and economy in 24-h scheduling. Guan et al. established necessary and sufficient conditions for feasible solutions under grid security constraints within a Lagrange relaxation framework. Yang et al. (2022) contributed to the deep integration of artificial intelligence and SCUC by developing a data-driven expert system based on an extended sequence-to-sequence (E-Seq2Seq) model. Through a multi-encoder-decoder architecture and dynamic sequence mapping, the system demonstrated high accuracy and strong generalization capability in real-world grid simulations in Hunan.

Currently, the significantly increased uncertainty in the power system prompts more researchers to focus on the flexibility and robustness of the SCUC problem. In the field of SCUC combined with energy storage system (ESS) scheduling, Zhao et al. (2025) proposed a multi-stage robust optimization method that significantly enhances the flexibility and computational efficiency of scheduling schemes. Holzer et al. (2025) focused on the aggregation modeling of Distributed Energy Resources (DERA) by developing a profit-maximization optimization model and a direct cost algorithm. Sharikabadi et al. (2024) considered the charging and discharging behaviors of electric vehicles, examining a flexibility-oriented approach for handling uncertain EVs in SCUC. For distribution networks with high penetration of renewable energy, Kim and Joo (2025) integrated the operational model of Mobile Virtual Power Lines (MVPL) into the SCUC framework, which improves operational flexibility while reducing renewable energy curtailment. Lu and Li (2024) proposed an enhanced Transmission Expansion Planning model considering climate impacts (TEP-CI) and developed a tailored SCUC model for affected grids, providing a systematic framework for future grid reliability assessment.

Existing studies on load forecasting and SCUC optimization predominantly treat load data as a single sequence for training, overlooking the differences in load fluctuation characteristics across various scenarios. To overcome this limitation, the present study proposes a data-driven framework that integrates load scenario clustering, fluctuation quantification, and SCUC optimization, with the goal of improving both load forecasting accuracy and unit commitment scheduling efficiency.

2 Methods

This study employs historical load data to quantitatively analyze load fluctuations across different time periods. The load power at each timestamp is clustered, and the fluctuation boundaries of these clusters at the subsequent timestep are investigated. A data-driven framework, built upon these boundaries, is proposed for load forecasting, enabling SCUC optimization scheduling based on the prediction results.

2.1 Clustering of different load scenarios

A set of 15 min-interval load power data is investigated, as shown in Figure 1a. Noting that the load power at different time periods has different fluctuation boundaries, represented by different confidence interval ranges. Generally speaking, during

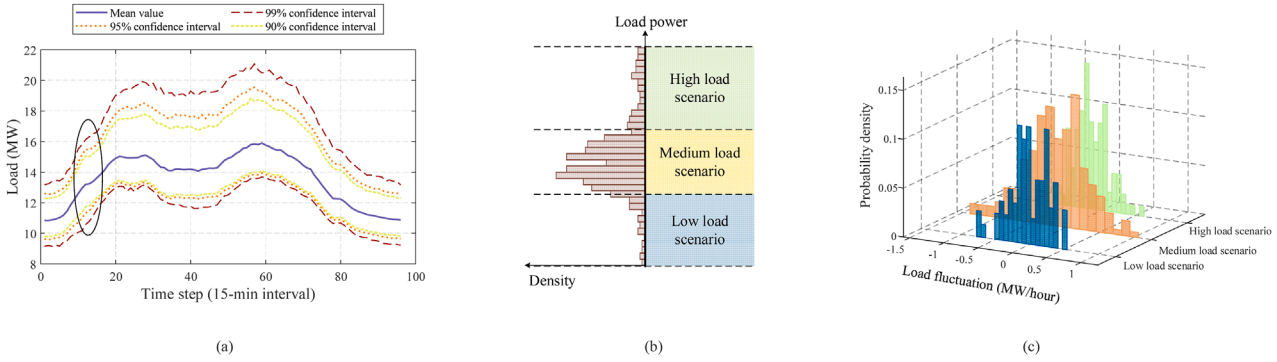

FIGURE 1
(a) Daily load power curves and the fluctuation boundaries. **(b)** Clustering for load scenarios. **(c)** Fluctuation distribution for three scenarios.

off-peak hours (e.g., at night), the average load is relatively low and exhibits a narrower fluctuation margin, which is reflected in the closely spaced boundaries of the 90%, 95%, and 99% confidence intervals. In contrast, during peak hours (e.g., daytime), the average load increases significantly and demonstrates greater volatility, making large-magnitude load fluctuations more likely to occur.

The load power distribution at the time instance selected by the circle in Figure 1A is analyzed, as shown in Figure 1b. The distribution of load power across different days of the year exhibits a unimodal shape. The distribution boundaries of the peak region are estimated using a 65% confidence interval, which ensures that both tail distributions retain sufficient probability and thereby enhances the reliability of the overall clustering result. The upper and lower bounds of this interval divide the entire probability distribution into three regions, designated as the low load scenario, medium load scenario, and high load scenario, as illustrated in Figure 1b. Based on the historical dataset, the magnitude of subsequent load fluctuations within each scenario is determined, and the differences are calculated to quantify the load fluctuation values. The load fluctuation distributions corresponding to these three scenarios are illustrated in Figure 1C.

Figure 1c depicts that the boundaries of fluctuation magnitudes differ under low, medium, and high load scenarios. Specifically, the fluctuation distributions under both low and high load scenarios are more concentrated, whereas the fluctuation range is wider under medium load scenarios.

These results can be explained as follows. Existing research (Chen et al., 2010) pointed out that the magnitude of load power is correlated with environmental factors such as temperature, humidity, and weather conditions. Among the three categories proposed in this study, the medium load scenario has the highest proportion, while high and low load scenarios are relatively less frequent. It can be inferred that medium load scenarios generally occur under common environmental conditions, whereas high and low load scenarios are caused by rare extreme external conditions. Due to inherent differences between common and extreme environmental conditions, the patterns of load fluctuations also differ under general versus extreme situations.

For example, under extreme conditions such as high-temperature weather, load power tends to remain at a high level since nearly all users utilize air conditioning. In such scenarios, electricity consumption behavior becomes more consistent across users, making abnormal fluctuations less likely to occur. In contrast, under normal conditions, external factors impose fewer constraints on user behavior, leading to greater uncertainty and unpredictability in load fluctuations. This analysis is reflected in the fluctuation boundaries of the load, showing more concentrated fluctuations under extreme scenarios.

2.2 Proposed data-driven framework

Section 2.1 indicates that different load scenarios correspond to different fluctuation boundaries and patterns. These fluctuation characteristics can be estimated using a data-driven approach combined with artificial neural networks. The specific process for quantifying load fluctuation features is described below.

1. Prepare the historical load power data and confirm the time interval T for load fluctuation quantization. We use the load power information of total T_L time to characterize the fluctuation level. Particularly, the T is set as 15 min and T_L is set as 1 h in this study.
2. Use the load power data from T_L time after current time to quantify the fluctuation level at current time. The fluctuation indicator is shown as Equation 1.

$$F(t) = \max_{i=t,\ldots,k+M-1} \left| P_{i+1}^L - P_t^L \right| + \sqrt{\frac{1}{M} \sum_{i=t}^{k+M-1} \left(P_{i+1}^L - P_i^L \right)^2} \quad (1)$$

Where $F(t)$ is the load fluctuation indicator at time t. P_t^L is the load power at time t. The parameter M is equal to $\frac{T_L}{T}$. This indicator contains two parts: 1) the maximum difference between the load power and the current value in M steps after time t; 2) the continuous fluctuation size of the load in M steps after time t. The higher the $F(t)$, the bigger the fluctuation level at time t. Compared to traditional fluctuation metrics such as standard deviation, the proposed F(t) incorporates both fluctuation boundaries and the rate of power

change. It not only captures the extent to which load power deviates from the mean but also more effectively reflects the underlying tendencies and characteristics of the fluctuations.

3. Obtain the fluctuation indicator $F(t)$ and verify its correctness. If valid, save the value. If not, initialize the calculation parameters and return to step 2.

Following the aforementioned calculation procedure, the fluctuation level can be quantified for the load data in each time interval. Therefore, based on the load clusters obtained at each time step using the method described in Section 2.1, the above procedure is applied to assign fluctuation indicators to different load levels within each cluster. These fluctuation indicators not only reflect differences in volatility level among load values within the same cluster but also capture the overall fluctuation tendency of the whole cluster. The load scenario clustering results and their corresponding fluctuation indicators at each time step are recorded as features in the historical dataset. This dataset is then used to train an artificial neural network to infer future load power fluctuation trends based on known load power information.

In traditional data-driven frameworks, only limited information such as date and weather are used as input features for the neural network. Once trained, the model can generate predictions based on available historical data. In contrast, the framework proposed in this paper builds upon traditional approaches by incorporating scenario clustering and load fluctuation features. This design offers the advantage of incorporating inherent factors influencing load fluctuations. It achieves improved prediction performance with acceptable training costs. This conclusion is supported by numerical experiments presented in Section 3.

Since the input load data exhibits temporal characteristics, the neural network used for generating predictions must be capable of processing sequential information. As a classic recurrent neural network architecture, the Long Short-Term Memory (LSTM) model is inherently designed to handle sequential data. It processes the input step-by-step sequentially and propagates historical information to subsequent time steps, thereby effectively capturing temporal dependencies. Therefore, the LSTM network was selected as the load forecasting model within the proposed framework in this study.

A typical LSTM architecture is illustrated in Figure 2, where x_t denotes the input at time step t, h_t represents the output at time step t, and c_t refers to the cell state of the LSTM at time t. The recurrent structure of the LSTM allows the state information to be propagated from one time step to the next, as shown in Figure 2a. The detailed structure of each LSTM cell is presented in Figure 2b, and the functions of these components are detailed in the figure caption. Each LSTM cell contains three gate layers: the forget gate, the input gate, and the output gate. The forget gate controls the extent to which information from the previous cell state is retained or discarded. It takes as input the previous output h_{t-1} and the current input x_t. The input gate regulates how much new information is incorporated into the cell state, thereby updating the cell state from c_{t-1} to c_t Finally, the output gate processes the current cell state c_t and produces the final output h_t through a weighted transformation.

In this study, the LSTM network takes the temporal features of load data as input. After processing through the hidden layers, the network outputs load forecasting results, which are then used for optimal UC scheduling.

2.3 Optimization model for unit commitment

Section 2.1 and Section 2.2 propose methods for load clustering and fluctuation quantification. Building on these methods, a data-driven framework is introduced for neural network training. According to the load forecasting results, a SCUC optimization model is developed to enhance the efficiency of unit commitment scheduling. The detailed formulation of the model is described below.

2.3.1 Objective function

$$min \sum_{g=1}^{NG} \sum_{t=1}^{NT} CF_{g,t} + CU_{g,t} + CD_{g,t} \tag{2}$$

Where g indicates the number of thermal unit and t indicates times. The maximum number of thermal units is defined as NG and NT is the number of time frames. $CF_{g,t}$ is the generation costs of thermal units. $CU_{g,t}$ and $CD_{g,t}$ are start-up and shut-down costs.

2.3.2 Generation costs constraints

$$CF_{g,t} = a_g\left(P_{g,t}^G\right)^2 + b_g P_{g,t}^G + c_g \tag{3}$$

Where a_g, b_g and c_g are coefficients of a quadratic function.

Using a piecewise function ϕ_m to linearize $CF_{g,t}$ into M segments:

$$CF_{g,t} = \max_{m \le M} \phi_m\left(P_{g,t}^G, u_{g,t}\right) \tag{4}$$

$$\phi_m\left(P_{g,t}^G, u_{g,t}\right) = K_m P_{g,t}^G + u_{g,t}\gamma_m \tag{5}$$

Where $\phi_m\left(P_{g,t}^G, u_{g,t}\right)$ indicates piecewise function of generation costs. K_m and γ_m represent the slope and intercept of the mth linear piece in the piecewise linear approximation. $u_{g,t}$ is the binary decision variable to indicate if thermal unit g turns on in period t.

2.3.3 Power balance constraints

$$\sum_{g=1}^{NG} P_{g,t}^G = \sum_{l=1}^{NL} P_{l,t}^L \tag{6}$$

Where $P_{l,t}^L$ indicates the forecasting load power of Bus l at time t. NL is the maximum number of load bus.

2.3.4 Thermal unit spinning reserve constraints

$$\sum_{g=1}^{NG} \left(u_{g,t}\overline{P_g^G} - P_{g,t}^G \right) \ge \rho \sum_{l=1}^{NL} P_{l,t}^L \tag{7}$$

Where $\overline{P_g^G}$ is the maximum output power of thermal unit g. ρ is the spinning reserve contribution factor.

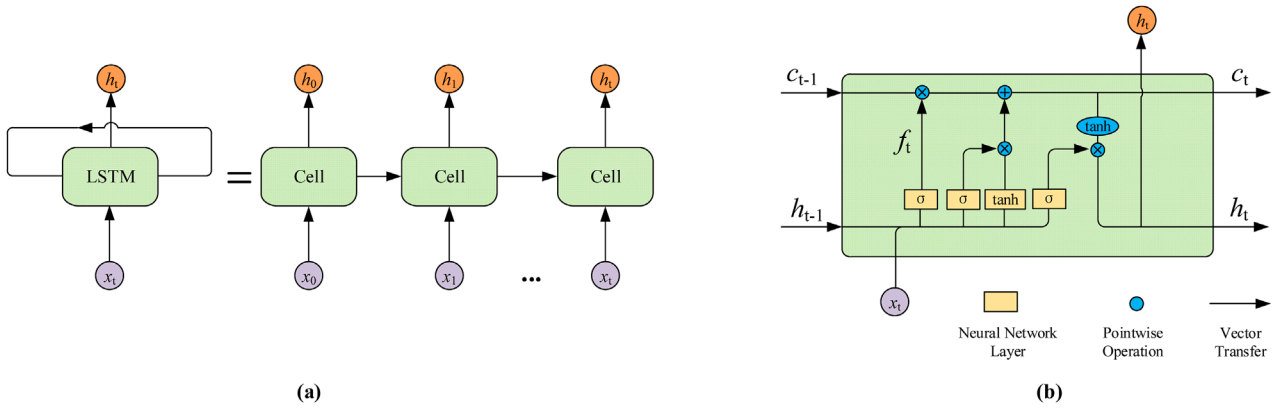

FIGURE 2
(a) LSTM network structure. **(b)** Internal structure for each LSTM cell.

2.3.5 Unit output power constraints

$$u_{g,t}\underline{P_g^G} \le P_{g,t}^G \le u_{g,t}\overline{P_g^G} \tag{8}$$

Where $\underline{P_g^G}$ is the minimum output power of thermal unit g.

2.3.6 Unit ramping and start-up/shut-down constraints

$$P_{g,t+1}^G - P_{g,t}^G \le u_{g,t}\left(RU_g - P_g^{SU}\right) + P_g^{SU} \tag{9}$$

$$P_{g,t+1}^G - P_{g,t}^G \ge -u_{g,t}\left(RD_g - P_g^{SD}\right) - P_g^{SD} \tag{10}$$

$$P_g^{SU} = P_g^{SD} = \frac{\left(\underline{P_g^G} + \overline{P_g^G}\right)}{2} \tag{11}$$

Where RD_g and RU_g are the maximum ramp-down and ramp-up speed of thermal unit g. P_g^{SU} and P_g^{SD} are maximum start-up and shut-down ramping power of unit g, respectively. Their values are calculated based on the average of the maximum and minimum output power of thermal unit g.

2.3.7 Minimum on/off duration time constraints

$$\sum_{k=t}^{t+TS_g-1}\left(1-u_{g,k}\right) \ge TS_g\left(u_{g,t-1}-u_{g,t}\right) \tag{12}$$

$$\sum_{k=t}^{t+TO_g-1} u_{g,k} \ge TO_g\left(u_{g,t}-u_{g,t-1}\right) \tag{13}$$

Where TS_g and TO_g are the minimum On/Off duration time of thermal unit g.

2.3.8 Start-up/shut-down cost constraints

$$\begin{cases} CU_{g,t} \ge SU_g\left(u_{g,t}-u_{g,t-1}\right) \\ CU_{g,t} \ge 0 \end{cases} \tag{14}$$

$$\begin{cases} CD_{g,t} \ge SD_g\left(u_{g,t}-u_{g,t-1}\right) \\ CD_{g,t} \ge 0 \end{cases} \tag{15}$$

Where SU_g and SD_g are the start-up and shut-down costs of thermal unit g.

2.3.9 Power flow security constraints

Using the DC power flow equations to approximate the non-convex and nonlinear branch power flow constraints:

$$\underline{P_{ij}} \le P_{ij} \le \overline{P_{ij}} \tag{16}$$

$$\sum_{i:i\to j} P_{ij} + \sum_j P_j^G = \sum_{k:j\to k} P_{jk} + P_j^L \tag{17}$$

$$P_{ij} = \frac{\theta_i - \theta_j}{x_{ij}} \tag{18}$$

Where P_{ij} is the branch power flow from Bus i to Bus j, which is constraint within the upper bound $\overline{P_{ij}}$ and lower bound $\underline{P_{ij}}$. x_{ij} is the branch reactance between Bus i and Bus j. θ_i is the phase angle of bus i. $\sum_{i:i\to j}P_{ij}$ represents the sum of all active power flowing from bus i to bus j.

The objective function Equation 2 with constraints Equation 3–18 can be formulated as a mixed integer linear programming (MILP) model. A commonly used solver CPLEX is employed to solve this model.

3 Results and discussion

3.1 Load forecasting results

As mentioned in Section 2.2, compared to traditional data-driven framework that does not consider scenario clustering or fluctuation characteristics, the data-driven framework proposed in this study offers the advantage of incorporating inherent factors affecting load fluctuations, thereby achieving improved prediction performance. The validity of this approach has been verified through numerical experiments in this section.

TABLE 1 Forecasting performance evaluation of two framework.

Methods	RMSE	MAE	MAPE	Training time (min)
Traditional framework	1.5957	1.1726	9.05%	58.17
Proposed framework	0.8292	0.6441	5.12%	67.28

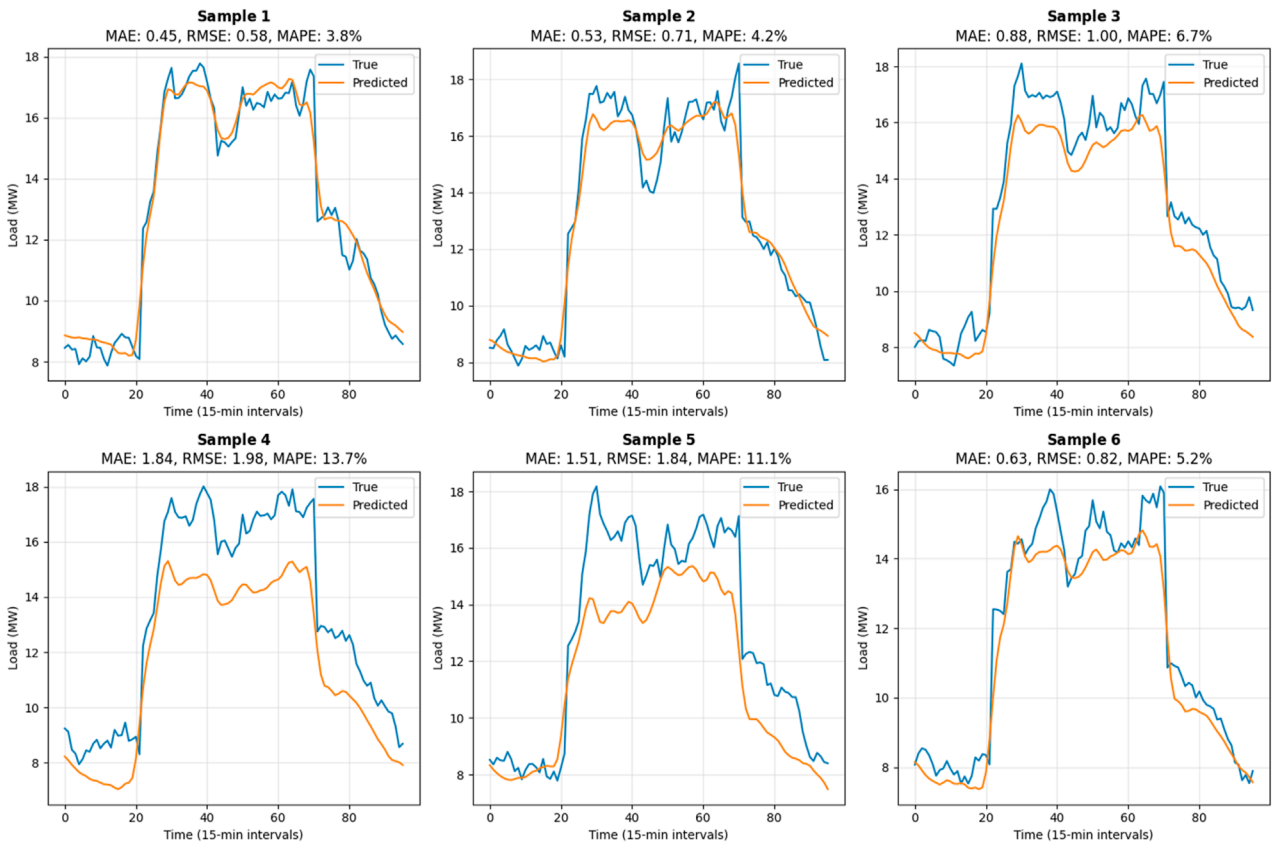

FIGURE 3
Prediction results of traditional framework.

To reduce the computational burden, the LSTM is configured with two layers and a hidden size of 128. A total of 366 days of historical data, with 96 points per day, is used for network training. The historical data is divided chronologically into training, testing, and validation sets in a ratio of 70%, 15%, and 15%, respectively. The LSTM network inputs 16 features derived from historical data and outputs prediction sequences of 96 steps. The network is trained using MSE as the loss function and the Adam optimizer at a learning rate of 0.001. Both the traditional data-driven framework and the proposed framework are used to train the LSTM neural network. The same set of 10 historical data samples is selected to evaluate the forecasting performance, and the results are presented in Table 1. The prediction results for the first six samples under the two frameworks are illustrated in Figures 3, 4.

Table 1 shows the average prediction errors of the two frameworks across 10 samples, measured by three metrics: Root Mean Square Error (RMSE), Mean Absolute Error (MAE), and Mean Absolute Percentage Error (MAPE). Compared to the traditional framework, the proposed framework achieves an average error reduction at 45.5%, i.e., 48.0% reduction in RMSE, 45.1% reduction in MAE, and a 43.4% reduction in MAPE. However, the increase in computational burden is only 15.7%. These results indicate that the proposed framework significantly improves the training effectiveness of the LSTM network with an acceptable computational overhead. This also demonstrates that the load scenario clustering and fluctuation indicator introduced in this study successfully capture and quantify temporal load fluctuation features into numerical results, revealing the underlying patterns of temporal fluctuation.

3.2 Unit scheduling planning

Based on the load forecasting results, the SCUC model proposed in Section 2.3 was validated on the IEEE 30-bus system (Deng et al.,

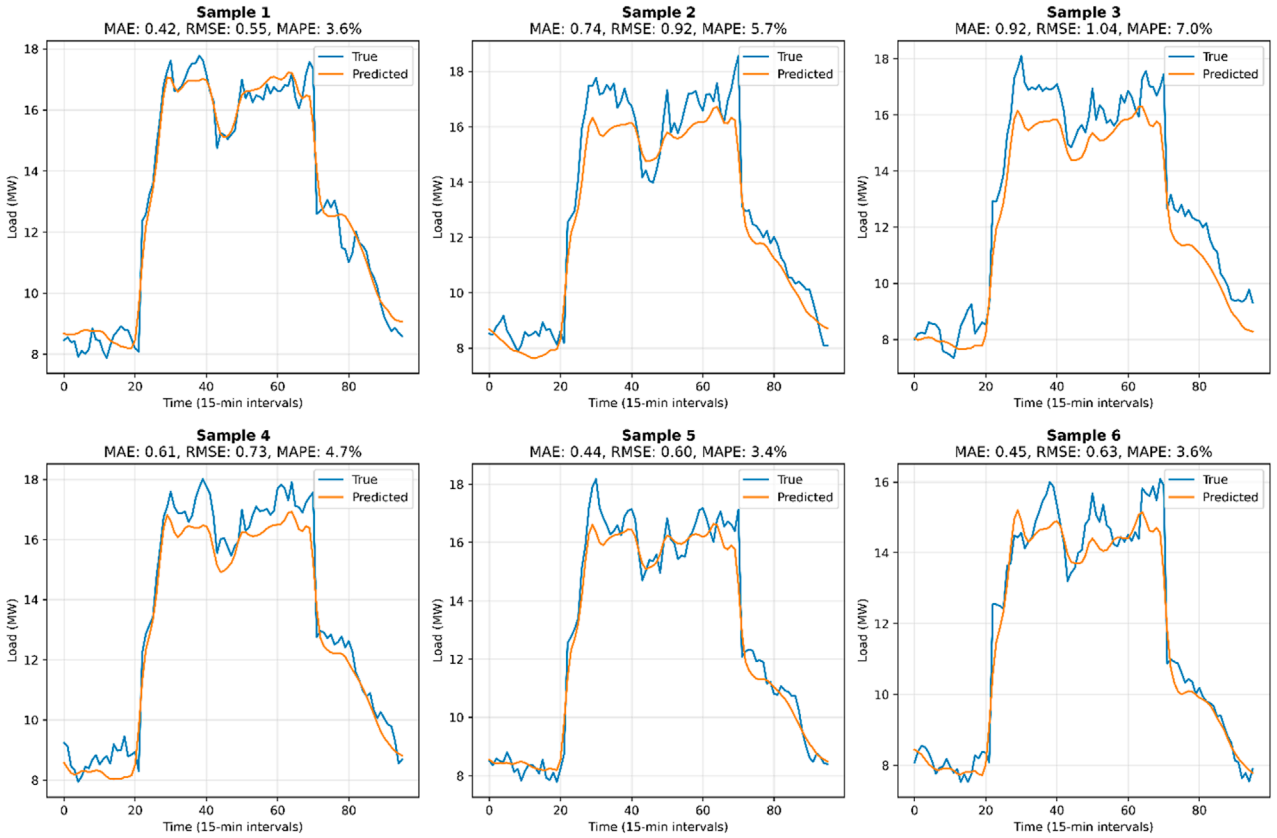

FIGURE 4
Prediction result of proposed framework.

TABLE 2 Calculation parameters for SCUC.

Unit number	Bus number	$\overline{P_g^G}$ (p.u.)	$\underline{P_g^G}$ (p.u.)	a_g/(p.u.)^2	b_g/p.u	c_g	RD_g/RU_g (p.u./h)	TS_g/TO_g (h)	SU_g ($/turns)	SD_g ($/turns)
1	1	1.50	0.50	0.1524	38.5397	786.799	0.1875	2	30,000	15,000
2	2	1.00	0.25	0.1058	46.1591	945.633	0.1000	2	25,000	12,500
3	5	0.60	0.15	0.0280	40.3965	1049.998	0.0750	2	15,000	7,500
4	8	0.80	0.50	0.0354	38.3055	1243.531	0.1000	2	20,000	10,000
5	11	0.40	0.10	0.0211	36.3278	1658.57	0.0750	2	10,000	5,000
6	13	0.40	0.10	0.0179	38.2704	1356.659	0.0750	2	10,000	5,000

2024). The computational parameters are listed in Table 2. With spinning reserve contribution factor ρ set to 0.10 and 0.20, the UC scheduling results are presented in Figure 5.

The scheduling results shown in Figure 5 can be interpreted as follows. From the perspective of generation cost, Unit 1 has the lowest cost, followed by Unit 2, Unit 3, and finally Unit 4. Therefore, as load demand increases, the units are dispatched sequentially in the order of Units 1, 2, 3, and 4. During peak load periods, all four units are required to operate simultaneously to meet the demand.

However, since the start-up/shut-down cost of Unit 3 is significantly lower than that of Unit 4, Unit 4 is activated earlier as shown in Figures 5a,b. In the combined output strategy of Units 2, 3, and 4, considering that Unit 2 has the largest quadratic cost coefficient while Units 3 and 4 have relatively smaller quadratic coefficients, Units 3 and 4 are prioritized to maintain high output levels. Unit 2 is assigned to regulate the total output of the UC system. During periods of significantly decreased load demand, Unit 2—which has the lowest start-up/shut-down cost—is shut down

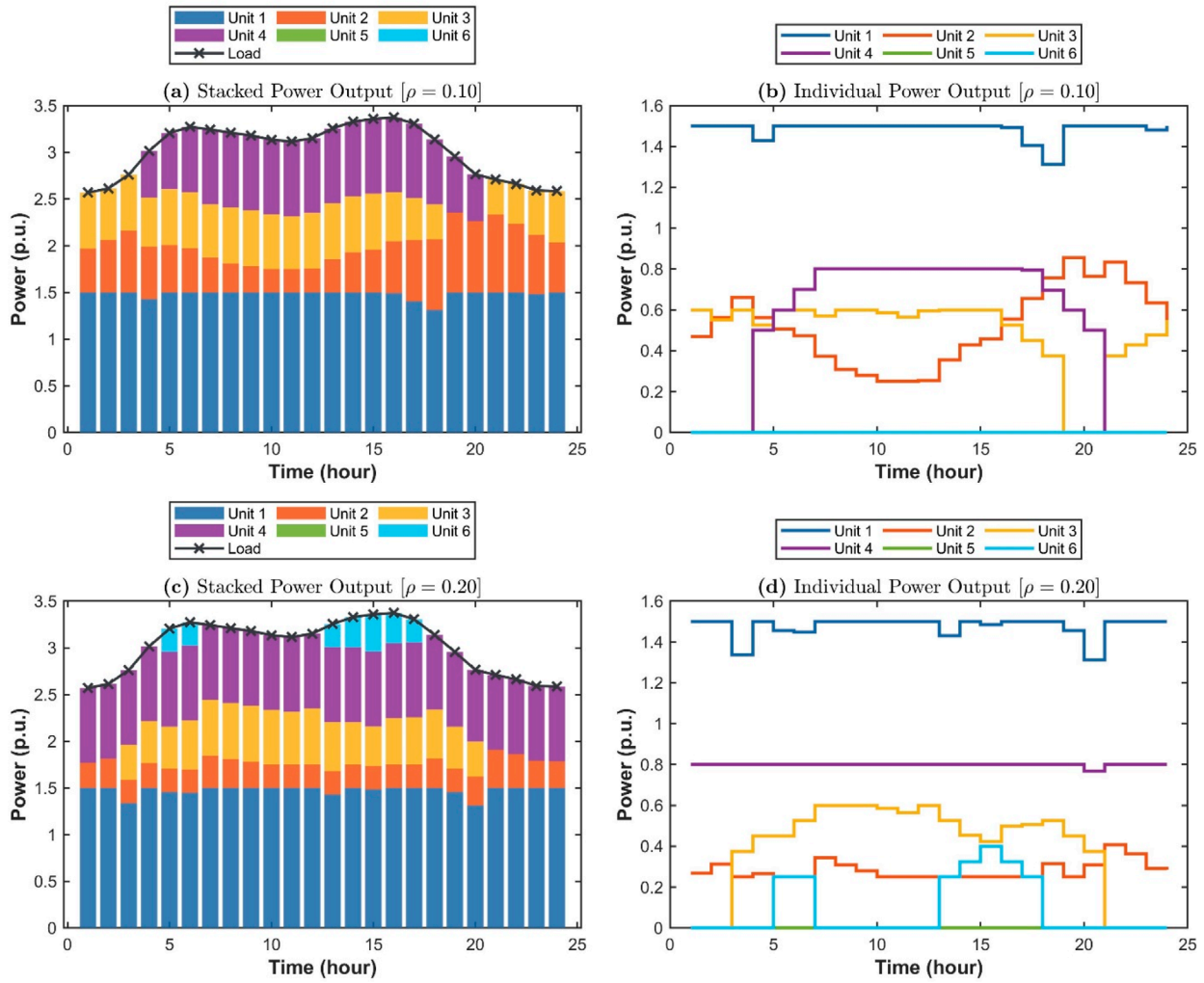

FIGURE 5
(a) Stacked power output and forecasted load power with ρ = 0.10. **(b)** Individual power output for each unit with ρ = 0.10. **(c)** Stacked power output and forecasted load power with ρ = 0.20. **(d)** Individual power output for each unit with ρ = 0.20.

TABLE 3 Forecasting performance evaluation of two framework.

Methods	Total cost (million$)	Solving time (s)
SCUC model from Dai et al.	8.864	25.14
Proposed SCUC model	8.926	18.81

first. After Unit 4 is shut down, Unit 2 is restarted simultaneously to maintain power balance.

Due to inherent errors in load forecasting, spinning reserve provided by the UC system is necessary to balance load fluctuations. Therefore, at least one unit remains capable of adjusting its output at any given time to ensure system stability. When increasing the spinning reserve, the UC scheduling results is shown in Figures 5c,d. During peak load periods, additional units must be activated to meet the demand for reserve capacity. The operating cost of Unit 6 is relatively lower compared to Unit 5, so Unit 6 is prioritized for dispatch. In Figure 5d, Unit 6 is started up between hours 5 and 7 to handle the rapid increase in load. Since Unit 3 has lower quadratic and linear generation cost coefficients than Unit 2, it is prioritized for ramping up during periods of increasing load, while Unit 2 is prioritized for reduction during decreasing load, as illustrated by the schedule results between hours 3 and 10 in Figure 5d. At hour 13, the load power rises again, necessitating the start-up of Unit 6 to meet the reserve capacity requirement. After Unit 6 is activated, the increased power output is preferentially allocated to it due to its smallest quadratic cost coefficient, which minimizes the cost associated with additional power generation. Correspondingly, the power output of Unit 3 is reduced since Unit 2 has already been adjusted to its minimum output level.

Compared with the SCUC model proposed by Dai et al. (2024), the model proposed in this paper improves both the formulation of the objective function and the minimum on/off duration time constraints. Additionally, the use of a DC power

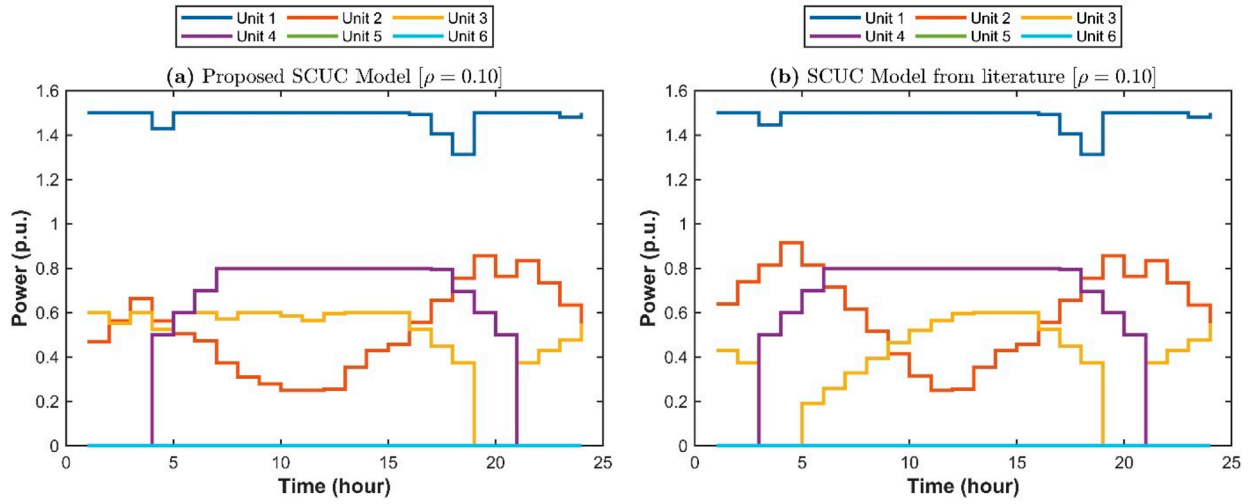

FIGURE 6
(a) Scheduling results computed by proposed SCUC model. **(b)** Scheduling results computed by SCUC model from (Dai et al., 2024).

flow approximation reduces unnecessary computational burden. The parameters of the model from (Dai et al., 2024) and those of our optimized model are kept consistent as shown in Table 2, and a comparison of the computational results is provided in Table 3.

Due to differences in the objective functions, the two models exhibit distinct optimization tendencies. Overall, while the optimization results of both models are similar, the proposed model requires shorter solution time and lower computational complexity. A detailed comparison of the unit commitment schedules is shown in Figure 6.

By comparing Figures 6a,b, it can be observed that the scheduling plan in Figure 6b exhibits more frequent units switching and larger variations in units' output. This is because the SCUC model proposed by Dai et al. (2024) places greater emphasis on minimizing total operational cost rather than start-up/shut-down expenses, resulting in a more aggressive UC schedule. This is reflected in the more frequent switching of Unit 3 and larger ramping magnitudes of Unit 2 and Unit 3. In contrast, the proposed model explicitly incorporates unit start-up/shut-down costs, resulting in a relatively conservative scheduling strategy. For instance, Unit 3 remains in operation during the third hour.

4 Conclusion

This paper proposed a data-driven framework to enhance the accuracy of load power forecasting and improve the optimization results of SCUC scheduling. Based on historical load data, the loads were categorized into three scenarios (low, medium, and high) using a 65% confidence interval. Differences in load fluctuation boundaries and characteristics were observed across these scenarios. Fluctuation indices are introduced to quantify the distinctive features under each scenario.

Compared to traditional data-driven approaches, the proposed data-driven framework reduces RMSE, MAE, and MAPE by 48.0%, 45.1%, and 43.4%, respectively, while only increasing training time by 15.7%. Computational experiments demonstrate that the proposed framework effectively captures temporal fluctuation patterns and overcomes the limitation of traditional methods that ignore inherent influencing factors. The results of case studies conducted on the IEEE 30-bus system validated the SCUC model constructed using the forecasting results of the proposed framework.

In future work, more efficient intelligent optimization algorithms could be integrated to further enhance the real-time performance and economic efficiency of SCUC scheduling, thereby offering a more comprehensive solution for power system operation under high penetration of renewable energy.

Data availability statement

The original contributions presented in the study are included in the article/supplementary material, further inquiries can be directed to the corresponding author.

Author contributions

SC: Conceptualization, Formal Analysis, Investigation, Methodology, Validation, Writing – original draft, Writing – review and editing. TF: Formal Analysis, Methodology, Validation, Writing – original draft, Writing – review and editing. HL: Formal Analysis, Validation, Visualization, Writing – original draft, Writing – review and editing. LH: Formal Analysis, Validation, Visualization, Writing – original draft, Writing – review and editing. YY: Investigation, Validation, Writing – original draft, Writing – review and editing.

ZW: Investigation, Validation, Writing – original draft, Writing – review and editing.

Funding

The author(s) declare that financial support was received for the research and/or publication of this article. This research was funded by science and technology program of Guizhou Power Grid Corporation, grant number 060000KC23110059 and the APC was funded by the same funding.

Conflict of interest

Authors SC, TF, HL, and LH were employed by China Southern Power Grid Guizhou Power Supply Co., Ltd. Authors YY and ZW were employed by Dongfang Electronics Co., Ltd.

Generative AI statement

The author(s) declare that no Generative AI was used in the creation of this manuscript.

Any alternative text (alt text) provided alongside figures in this article has been generated by Frontiers with the support of artificial intelligence and reasonable efforts have been made to ensure accuracy, including review by the authors wherever possible. If you identify any issues, please contact us.

Publisher's note

References

Abumohsen, M., Owda, A. Y., and Owda, M. (2023). Electrical load forecasting using LSTM, GRU, and RNN algorithms. *Energies* 16, 2283. doi:10.3390/en16052283

Chen, Y., Luh, P. B., Guan, C., Zhao, Y., Michel, L. D., Coolbeth, M. A., et al. (2010). Short-term load forecasting: similar day-based wavelet neural networks. *IEEE Trans. Power Syst.* 25, 322–330. doi:10.1109/TPWRS.2009.2030426

Chen, Y., Wang, F., Ma, Y., and Yao, Y. (2020). A distributed framework for solving and benchmarking security constrained unit commitment with warm start. *IEEE Trans. Power Syst.* 35, 711–720. doi:10.1109/TPWRS.2019.2930706

Dai, J., Tian, N., Zhao, Q., Tang, C., Xuan, P., and Cheng, L. (2024). An ADMM approach for unit commitment with considering dynamic line rating. *Front. Energy Res.* 12, 1479347. doi:10.3389/fenrg.2024.1479347

Deng, M., Liu, Y., Hong, Y., Sun, Z., and Hao, J. (2024). Study on the grid supporting effects for GFM energy storage system in distribution networks under grid faults. *Energy Rep.* 12, 5801–5813. doi:10.1016/j.egyr.2024.11.063

Fu, Y., Shahidehpour, M., and Li, Z. (2006). AC contingency dispatch based on security-constrained unit commitment. *IEEE Trans. Power Syst.* 21, 897–908. doi:10.1109/TPWRS.2006.873407

Fu, Y., Li, Z., and Wu, L. (2013). Modeling and solution of the large-scale security-constrained unit commitment. *IEEE Trans. Power Syst.* 28, 3524–3533. doi:10.1109/TPWRS.2013.2272518

Guan, X., Guo, S., and Zhai, Q. (2005). The conditions for obtaining feasible solutions to security-constrained unit commitment problems. *IEEE Trans. Power Syst.* 20, 1746–1756. doi:10.1109/TPWRS.2005.857399

Holzer, J., Cornachione, M., Li, L., Schweitzer, E., and Eldridge, B. (2025). Modeling distributed energy resource aggregations in security constrained unit commitment and economic dispatch. *Int. J. Electr. Power Energy Syst.* 170, 110727. doi:10.1016/j.ijepes.2025.110727

Khuntia, S. R., Rueda, J. L., and van der Meijden, MAMM (2016). Forecasting the load of electrical power systems in mid- and long-term Horizons: a review. *IET Gener. Transm. Distrib.* 10, 3971–3977. doi:10.1049/iet-gtd.2016.0340

Kim, S., and Joo, S.-K. (2025). Spatiotemporal operation method for Mobile virtual power line in power system with mobile energy storage systems. *J. Energy Storage* 108, 115196. doi:10.1016/j.est.2024.115196

Li, Y., Bu, F., Li, Y., and Long, C. (2023). Optimal scheduling of island integrated energy systems considering multi-uncertainties and hydrothermal simultaneous transmission: a deep reinforcement learning approach. *Appl. Energy* 333, 120540. doi:10.1016/j.apenergy.2022.120540

Li, Y., Ma, W., Li, Y., Li, S., Chen, Z., and Shahidehpour, M. (2025). Enhancing cyber-resilience in integrated energy system scheduling with demand response using deep reinforcement learning. *Appl. Energy* 379, 124831. doi:10.1016/j.apenergy.2024.124831

Lin, J., Ma, J., Zhu, J., and Cui, Y. (2022). Short-term load forecasting based on LSTM networks considering attention mechanism. *Int. J. Electr. Power Energy Syst.* 137, 107818. doi:10.1016/j.ijepes.2021.107818

Liu, M., Kong, X., Xiong, K., Wang, J., and Lin, Q. (2025). Multi-scale spatio-temporal transformer: a novel model reduction approach for day-ahead security-constrained unit commitment. *Appl. Energy* 380, 124963. doi:10.1016/j.apenergy.2024.124963

Lu, J., and Li, X. (2024). Transmission expansion planning for renewable-energy-dominated power grids considering climate impact. *J. Mod. Power Syst. Clean. Energy* 12, 1737–1748. doi:10.35833/MPCE.2023.000990

Rafi, S. H., Deeba, S. R., and Hossain, E. (2021). A short-term load forecasting method using integrated CNN and LSTM network. *IEEE Access* 9, 32436–32448. doi:10.1109/ACCESS.2021.3060654

Sharikabadi, R., Abdollahi, A., Rashidinejad, M., and Shafiee, M. (2024). Security constrained unit commitment in smart energy systems: a flexibility-driven approach considering false data injection attacks in electric vehicle parking lots. *Int. J. Electr. Power Energy Syst.* 161, 110180. doi:10.1016/j.ijepes.2024.110180

Tang, X., Chen, H., Xiang, W., Yang, J., and Zou, M. (2022). Short-term load forecasting using channel and temporal attention based temporal convolutional network. *Electr. Power Syst. Res.* 205, 107761. doi:10.1016/j.epsr.2021.107761

Tian, Z., Liu, W., Jiang, W., and Wu, C. (2024). CNNs-transformer based day-ahead probabilistic load forecasting for weekends with limited data availability. *Energy* 293, 130666. doi:10.1016/j.energy.2024.130666

Wan, A., Chang, Q., Al-Bukhaiti, K., and He, J. (2023). Short-term power load forecasting for combined heat and power using CNN-LSTM enhanced by attention mechanism. *Energy* 282, 128274. doi:10.1016/j.energy.2023.128274

Wang, Y., Gan, D., Sun, M., Zhang, N., Lu, Z., and Kang, C. (2019). Probabilistic individual load forecasting using pinball loss guided LSTM. *Appl. Energy* 235, 10–20. doi:10.1016/j.apenergy.2018.10.078

Wang, Y., Chen, J., Chen, X., Zeng, X., Kong, Y., Sun, S., et al. (2021). Short-term load forecasting for industrial customers based on TCN-LightGBM. *IEEE Trans. Power Syst.* 36, 1984–1997. doi:10.1109/TPWRS.2020.3028133

Wang, C., Wang, Y., Ding, Z., Zheng, T., Hu, J., and Zhang, K. (2022). A transformer-based method of multienergy load forecasting in integrated energy system. *IEEE Trans. Smart Grid* 13, 2703–2714. doi:10.1109/TSG.2022.3166600

Xu, M., and Zhuan, X. (2013). Optimal planning for wind power capacity in an electric power system. *Renew. Energy* 53, 280–286. doi:10.1016/j.renene.2012.11.015

Yang, N., Yang, C., Wu, L., Shen, X., Jia, J., Li, Z., et al. (2022). Intelligent data-driven decision-making method for dynamic multisequence: an E-Seq2Seq-based SCUC expert system. *IEEE Trans. Ind. Inf.* 18, 3126–3137. doi:10.1109/TII.2021.3107406

Zhao, J., Zhai, Q., Zhou, Y., and Cao, X. (2025). An analytical feasibility condition for the multi-stage robust scheduling of energy storage systems with application on SCUC. *IEEE Trans. Power Syst.* 40, 435–448. doi:10.1109/TPWRS.2024.3404503

Zheng, H., Yuan, J., and Chen, L. (2017). Short-term load forecasting using EMD-LSTM neural networks with a xgboost algorithm for feature importance evaluation. *Energies* 10, 1168. doi:10.3390/en10081168